Published in final edited form as:
Analyst. 2013 November 21; 138(22): 6986–6996. doi:10.1039/c3an36819j.

Differential proteomic analysis of caveolin-1 KO cells reveals Sh2b3 and Clec12b as novel interaction partners of caveolin-1 and capns1 as potential mediator of caveolin-1-induced apoptosis

Yogesh M Kulkarni[a,1], **Changxing Liu**[b,1], **Qi Qi**[b], **Yanmei Zhu**[b], **David J Klinke**[a,b,*], and **Jun Liu**[b,c,*]

[a]Department of Chemical Engineering, College of Engineering and Mineral Resources, Morgantown, West Virginia, 26506, U.S.A.

[b]Mary Babb Randolph Cancer Center, West Virginia University, Morgantown, West Virginia, 26506, U.S.A.

[c]Department of Physiology and Pharmacology, School of Medicine, West Virginia University, Morgantown, West Virginia, 26506, U.S.A.

Abstract

Caveolin-1 (Cav1) is a small scaffolding protein implicated in a variety of cellular functions, including cell signaling, lipid transport and membrane traffic. The objective of this study was to use comparative proteomics to identify differentially expressed proteins in Cav1 knockout (KO) mouse embryonic fibroblasts. These deregulated proteins were then analyzed using systems biology tools to gain insight into the local network properties and to identify the interaction partners of Cav1. We identified five proteins that were up-regulated and ten proteins that were down-regulated in Cav1 KO cells, suggesting that the local network behaves as a complex system. Protein interaction network analysis revealed two proteins, Sh2b3 and Clec12b, as novel interaction partners of Cav1. Functional annotation showed apoptosis signaling as the most significant pathway. To validate this functional annotation, Cav1 KO cells showed more than 1.5-fold increase in caspase-3 activity over wild type cells upon apoptotic stimulation. We also found that calpain small subunit 1 is up-regulated in Cav1 KO cells and directly influences cell response to apoptotic stimuli. Moreover, Capns1 was reduced in Cav1 KO cells following re-expression of Cav1 and suppression of Capns1 activity in Cav1 KO cells significantly inhibited the sensitivity to apoptotic stimuli, as measured by caspase 3 activity. In conclusion, our results suggest that Sh2b3 and Clec12b functionally interact with Cav1 and that calpain small subunit 1 may mediate Cav1-induced apoptosis.

[*]Co-corresponding authors: Jun Liu, M.D.,Ph.D. Mary Babb Randolph Cancer Center, West Virginia University, One Medical Center Dr., West Virginia University, PO Box 9229, Morgantown, West Virginia, 26506. Tel: (304) 293-1503; Fax: (304) 293-3850; junliu@hsc.wvu.edu, David Klinke, PhD. Department of Chemical Enginerring, College of Engineering and Mineral Resources, Morgantown West Virginia, 26506. David.Klinke@mail.wvu.edu.
[1]These authors contributed equally to this work

Competing interests
The authors declare no competing financial interests.

Keywords

proteomics; caveolin-1; calpain small subunit 1; apoptosis; Sh2b3; Clec12b

INTRODUCTION

Caveolin-1 is the major structural protein of caveolae, a form of plasma membrane microdomain,, that are involved in a variety of cellular functions, including lipid transport, membrane trafficking, and cell signaling [1–4]. Mammalian caveolin-1 (Cav1) is one of three isoforms that exhibit differential expression. Cav1 and Cav2 are abundantly expressed in many kinds of cells, such as endothelial cells and fibroblasts, whereas Cav3 expression is restricted to muscle tissue [5,6]. In the context of cell signaling, Cav1 has a 20 aa motif (aa 82–101), [7,8] that interacts with many signaling proteins including Src family kinases, Gα subunits, H-Ras, protein kinase C, endothelial Nitric Oxide Synthase, PI3-kinase, integrins, EGF-receptor and VEGF-receptor[9–12] thereby leading to target protein inactivation[9]. This implies that Cav1 functions as an endogenous negative regulator of many signaling molecules. Consistent with the notion that Cav1 plays important roles in cellular transport and signal transduction, Cav1 knockout mice showed several pathological phenotypes, including lung fibrosis, concentric left ventricular hypertrophy and right ventricular dilation, resistance to diet-induced obesity, increased ischemic injury, and enhancement of tumor formation and metastasis, suggesting that Cav1 has pleiotropic functions in various organs[13]. Identifying the specific roles that Cav1 plays in these different membrane transport and signal transduction processes remains a challenge.

A classical approach to identify a function of an element is to remove the element and observe its functional consequences on the system. In biological context, this simply translates to knocking out a gene from a cell and using the resulting phenotype to identify its exact role in the cellular context [14]. This technique has been used in its simplest form by knocking out a single gene to decipher its function or used in large scale efforts to knock-out genes systematically, using shRNA libraries or genetic engineering, to decipher the function of all genes encoded by the mammalian genome to aid in drug discovery and validation [15–17]. Identifying gene function by knockout is based upon the assumption that observed result or difference is a causal effect of the removal of gene alone and nothing else. This classical reductionist approach of removing one gene at a time to study its role in the cellular context is predicated on the assumption that a cell is a *simple* or a *complicated* system. A simple system has a small number of components with well defined roles, such as a pendulum that is governed by Newton's laws of motion. In comparison, a complicated system has a large number of components that each have well defined roles and interact through a set of well defined rules [18]. Engineered systems, such as an electronic circuit, are examples of a complicated system. A common view has been to think of cell signaling pathways as electronic circuits that transduce signals along pathways depicted using wiring diagrams [19,20]. Gene knockout in the context of a circuit perspective implies that when a node is removed, the remaining network is unaltered.

A biological cell on the other hand may be considered a *complex* system, which is defined by [18]Amaral and Ottino (2004) as having a large number of components interacting according to rules that may change over time and that may not be well understood. In the context of a cell, these components include proteins that interact and, through post-translational modifications, transmit information. In a complex system, the flow of information among the components can be plastic and the roles that proteins play in regulating this flow may be fluid. As a cell dynamically adapts to changes in its environment, an alternative view of cellular signaling networks is that they are also complex systems, as proteins dynamically assemble into multi-protein complexes. The molecular composition of such complexes provides specificity in directing the flow of information; alterations in the composition of the complex may redirect the flow down competing pathways [21]. Gene knockout in the context of a circuit perspective implies that a node is removed but the remaining network is unaltered. In the context of a complex signaling network, deleting a node from a network will perturb the neighboring interconnected nodes and will cause a ripple effect throughout the network. The effect of the node removal will depend on the connectivity of the node within the network and the collective response of the network to perturbations [22]. [20].

Given the expected behaviors for knocking out a gene in simple, complicated, and complex systems, the objective of the study was to gain insight on the molecular pathways affected by the depletion of Cav1. Towards this aim, we compared the proteome of Cav1 KO mouse embryonic fibroblasts (MEFs) with the proteome of wild type MEFs using two-dimensional electrophoresis (2-DE) and MALDI-TOF MS based workflow. We analyzed the differentially expressed proteins using systems biology tools to obtain a system-level understanding of the molecular pathways affected by Cav1 depletion and to identify the potential interaction partners for Cav1. In short, our data suggest that the observed system behaves as a complex system, as suggested by a number of identified proteins that exhibited altered abundance in cells lacking Cav1.

EXPERIMENTAL

Cell culture

Primary cultured fibroblasts were obtained from Day 13.5 mouse embryos of wild-type and Cav1 knockout mice as previously described [33] according to the WVU ACUC approved protocol. Mouse embryonic fibroblasts (MEFs) were cultured in DMEM (Dulbecco's modified Eagle's medium, Life Technologies, Inc.) supplemented with 10% fetal bovine serum (FBS), 2 mM glutamine, 100 units/ml penicillin and 100 μg/ml streptomycin in a humidified incubator at 37 °C and 5% (v/v) CO_2.

Sample preparation for 2-D electrophoresis

Sample preparation for 2DE was done as we have previously described [46]. Briefly, cells were incubated in lysis buffer (7M Urea, 2M thiourea, 2 % (w/v) CHAPS) for 30 min on ice and sonicated for five cycles in an ultrasonic water bath, where each sonication was performed for 30 s followed by 30 s cooling interval on ice. Cell debris were pelleted by centrifugation at 14,000 rpm for 40 min at 4 °C. The supernatant was aliquoted in fresh

tubes and stored at −80 °C. The protein concentration was determined using CB-X™ protein assay (G Biosciences).

2-D Electrophoresis

For each cell line, 120 μg of cell lysate was mixed with rehydration buffer (7M urea, 2M thiourea, 2% CHAPS, 1% DTT, 2% IPG buffer, 0.002% bromophenol blue) and incubated for 1 h at room temperature prior to rehydration on Immobilized pH Gradient (IPG) strips pH 4–7, 7 cm, (GE Healthcare, Uppsala, Sweden) for 12 h at 25 °C. Isoelectric focusing was done using Ettan IPGphor apparatus (Amersham Biosciences) for a total of 17 kVh at 50 μA per strip. Focused IPG strips were equilibrated in 1% (w/v) DTT followed by 2.5% (w/v) iodoacetamide before transferring onto 12% SDS-polyacrylamide gel. The coomassie stained gels were scanned using Typhoon 9400 scanner (Amersham Biosciences) at 100 μm resolution at normal sensitivity. Data were saved in .gel format using ImageQuant software (Amersham Biosciences). Three technical replicates were acquired for each primary cell type.

Image analysis

The images corresponding to all three 2DE replicates for both the WT and Cav1 K.O. cell types were collectively analyzed using REDFIN Solo software from Ludesi. Gel images were cropped to remove the boundary region without proteins. The warping was done by choosing a reference image and spot matching was facilitated by placing approximately 10 manual vectors in each quadrant of the gel to align cognate spots at corresponding locations across different gels. Normalized spot volumes were generated from the optical densities for each individual spot to the ratio of the total spot volume in each gel. Spots considered for subsequent analysis had to be present in at least three of the six gels. In addition, protein spots were considered to be differentially expressed if the difference between the averages of spot densities from the Cav1 KO and WT MEFs was 1.5-fold or greater with $p<0.05$, as assessed using an ANOVA test.

In-gel digestion

The manually excised gel spots of interest were destained in 50–50% acetonitrile/50mM NH_4HCO_3 solution, reduced in DTT (100mM, 57 °C, 45 min) and alkylated with iodoacetamide (500mM, room temperature, 45 min) in a dark room. The gel pieces were dehydrated in acetonitrile for 10 min, were vacuum dried and rehydrated with 10 μL of digestion buffer (10ng/μL of trypsin (Promega; Madison, WI) in 50mM NH_4HCO_3) and covered with 10 μL of NH_4HCO_3. The samples were incubated for 16 h at 37 °C to allow for complete digestion. 5% formic acid was added to stop the enzymatic digestion and the peptides were extracted in sequential steps by sonication using acetonitrile and 50% acetonitrile/0.1% TFA.

MALDI-TOF MS analysis

MALDI-TOF-MS system model Micromass MALDI-R (Waters®) was used to obtain the peptide mass fragment spectra as recommended by the manufacturer. Protein digest solutions were mixed at a 1:1 ratio with the MALDI matrix α-cyano-4-hydroxycinnamic

acid (CHCA) (Sigma–Aldrich Fluka; St. Louis, MO). 2 μL of tryptic digest was applied to the MALDI plate and allowed to dry. The MALDI-TOF MS was operated in the positive ion delayed extraction reflector mode for highest resolution and mass accuracy. Peptides were ionized/desorbed with a 337-nm laser and spectra were acquired at 15 kV accelerating potential with optimized parameters. The external calibration performed using ProteoMass Peptide MALDI-MS Calibration Kit (Sigma) provided mass accuracy of 25–50 ppm. Internal calibration was performed with the monoisotopic peaks of Angiotensin II (*m/z*: 1046.5423), $P_{14}R$ (synthetic peptide) (*m/z*: 1533.8582) and adrenocorticotropic hormone (ACTH) (18–39) peptide (*m/z*: 2465.1989). Mass spectral analysis for each sample was based on the average of 800–1000 laser shots. Peptide masses were measured from *m/z*: 800 to 3,000. The raw spectra was background subtracted, smoothed and deisotoped using ProteinLynxGlobalServer (PLGS) v2.1. The peak lists containing the *m/z* ratio and corresponding intensity values were exported to Microsoft Excel for further processing.

Protein identification using peptide mass fingerprinting (PMF)

Peptide mass fingerprint's (PMF) obtained from MALDI-TOF MS were used to query public protein primary sequence databases for protein identification. Monoisotopic peaks resulting from internal calibrants were removed before submitting the peak lists to the databases. Mascot database search engine v2.3.02 (www.matrixscience.com, Matrix Science Ltd., UK) and Expasy Aldente (version 19/03/2010) were used to query the UniProtKB/Swiss-Prot human database (Release 2010_12, 523151 sequences, 184678199 amino acids) with the following settings: peptide mass tolerance of 50 ppm, one missed cleavage site, one fixed modification of carboxymethyl cysteine, one variable modification of methionine oxidation, minimum of four peptide matches and no restrictions on protein molecular mass (MW) or isoelectric point (pI). A protein was considered to be positively identified only when it was a hit using both algorithms.

Ingenuity pathway Analysis

Differentially regulated proteins identified by 2DE and PMF were further analyzed using Ingenuity Pathway Analysis (IPA; Ingenuity Systems, Mountain View, CA; www.ingenuity.com). IPA was used to interpret the differentially expressed proteins in terms of an interaction network and predominant canonical pathways as described in detail earlier [46]. Briefly, a dataset containing the differentially regulated proteins, called the focus proteins, for a particular cell line was uploaded into the IPA. These focus proteins were overlaid onto a global molecular network developed from the information in the IKB. Networks of these focus proteins were then algorithmically generated by including as many focus proteins as possible and other non-focus proteins from the IKB that are needed to generate the network based on connectivity. Enriched canonical pathways were identified from the IPA library using a Fisher's exact test adjusted for multiple hypothesis testing using the Benjamini-Hochberg correction [47]. A low p-value suggests that the pathways associated with the differentially expressed proteins were not observed by random chance alone.

Immunoblot analysis

Using an independent samples from the proteomic analysis, the expression levels of proteins were determined by Western blot analysis. Wild-type and Cav1 KO MEFs were seeded in 6-cm dishes, lysed in ice-cold lysis buffer containing 1.0% Triton X-100, 60mM Octylglucoside, and 1mM PMSF supplemented with protease inhibitors. Protein concentration was determined using BCA™ protein assay kit (Thermo Scientific). 20μg proteins were separated by SDS-PAGE on a 15% gel, electro-transferred to a nitrocellulose membrane, and immunoblotted against either Cav1 (Santa Cruz Biotech) or calpain small subunit 1 (Capns1, Aviva Systems Biology). The membranes were reprobed with antibody against GAPDH.

Apoptosis assay

MEFs were treated with 1 μM staurosporine. Caspase 3-like activity was determined using caspase 3 fluorescent assay kit as previously described [42]. Briefly, after treatment with staurosporine, incubation medium was removed and the cells were lysed for 10 min in ice-cold lysis buffer containing 20 mM Tris-HCl (pH 7.4), 137 mM NaCl, 1% Nonidet P-40, 10% glycerol, 1 mg/ml aprotinin, 1 mM leupeptin, and 1 mM PMSF. Total cell lysates (10 μg each) were incubated at 37°C for 60 min in enzyme assay buffer containing 20 mM Hepes (pH 7.5), 10% glycerol, 2 mM DTT, 1 mM PMSF, and 100 μM caspase 3 substrate, *N*-acetyl-Asp-Glu-Val-Asp (DEVD)-7-amino-4-methyl coumarin (AMC). The reaction was terminated by adding 1 ml of deionized H_2O. Fluorescence was measured using Fluostar Optima (BMG Labtechnologies, Inc.) equipped with a 380-nm excitation filter and a 460-nm emission filter.

Adenovirus production and infection

Adenovirus encoding full-length Cav-1 (AdCav1-GFP) or GFP (AdGFP) were produced and used to infect cells as we described previously with some modifications [33]. Briefly, Cav1 KO MEFs were grown in DMEM supplemented with 10% FBS. When cells became 70% confluent, a mixture of polybrane and either AdCav1-GFP (50 pfu) or AdGFP (50 pfu) was added into growth medium, and incubated with the cells for 24 hours. At the end of incubation, cells were washed once with PBS, lysed in lysis buffer containing 10 mM Tris-HCl (pH=7.4), 0.15 M NaCl, 1% Triton X-100, 60 mM octylglucoside and protease inhibitors and used for immunoblot analysis.

Statistical Analysis

Data are presented as mean ± S.D. Statistical analysis was performed using Student's *t* test. A *p*-value of <0.05 was considered statistically significant.

RESULTS

2DE and Image Analysis

Two-dimensional gel electrophoresis (2DE) was used to assess global alterations in protein abundance between wild type and Cav1 KO mouse embryonic fibroblasts (MEFs). The highly reproducible qualitative pattern of cellular proteome obtained in the pH range 4–7

after 2DE of total cellular extracts for three technical replicates of Cav1 KO and WT MEFs is shown in Figure 1A. Each group had more than 1,300±3 unique protein spots resolved indicating an equal amount of protein load on each replicate (Figure 1B). Coomassie Blue G-250, dubbed “blue silver”, was used for staining the gels due to its high sensitivity approaching that of conventional silver staining, as was evident in our study from the dynamic range of the normalized protein spots spanning four orders of magnitude [21]. The normalized intensities of matching spots for each group were plotted as a scatter plot on a logarithmic scale indicating a strong correlation between normalized intensities and a dynamic range of detection spanning four orders of magnitude (Figure 1C). Colloidal Densitometric quantification of relative spot intensities in the KO and WT fibroblasts revealed a total of 16 spots that were well-resolved and showed a significant ($p< 0.05$) difference in expression by at least 1.5-fold (Figure 2A). An example of a well-resolved protein spot with its presence in each gel across both groups (Figure 2B) and the normalized volume of the spot in each gel with the fold-change and significance (Figure 2C) are shown.

Peptide Mass Fingerprinting

The differentially expressed protein spots were excised, in-gel digested by trypsin and analyzed by MALDI-TOF MS to generate a peptide mass fingerprint. The resulting peptide mass fingerprints were queried against the Swiss-Prot human database using Mascot as a primary database search algorithm. Expasy Aldente was used as a complementary algorithm for additional confirmation to reduce the possibility of false positive identification. Two independent algorithms were used for identification to consolidate the identification through complementary features of these packages, where Aldente has a distinct advantage over Mascot by its ability to identify modified protein isoforms. Agreement between the apparent M_r and pI observed on the 2-D gel and the theoretical values of the identified proteins, number of peptide matches and sequence coverage provided additional support for positive identification. Peptide mass fingerprint with the tryptic peptide mass values that contributed towards identification of calpain small subunit 1 (Capns1) is exemplified in Figure 2D. From 16 picked spots, 15 differentially expressed proteins were identified, from which 10 proteins were down-regulated and 5 proteins were up-regulated in KO MEFs (Table 1; Supplemental File 1). One spot could not be identified unambiguously and was therefore excluded from any further analysis. More than 85% of the spots had sequence coverage exceeding 25%. These differentially expressed proteins (Table 1; Supplemental File 1) formed the dataset for pathway analysis and network generation. Protein spots with shifts in their pI but identical MW may correspond to the isoforms of the same protein, which might be a result of post translational modifications, but is more common in 2-DE due to the inherent artifacts in 2-DE protocol. Urea in the lysis buffer causes carbamylation of proteins causing a significant shift in the pI of the protein. This was evident in the case of a protein spot identified as cytoplasmic actin, where the observed pI of the protein was found to be 6.8 as compared to the theoretical pI of 5.3.

Pathway analysis and protein interaction network generation using IPA

Using the observed patterns of proteins that were differentially expressed, we annotated the patterns with biological function by quantifying biological pathways that were enriched in the data set from all the canonical pathways contained within the IPA library. In addition,

the ratio of observed proteins relative to the total number of proteins in a pathway provided an additional metric for pathway enrichment. The results from this pathway analysis are summarized in Figure 3. The proteins that were either up-regulated (Figure 3A) or down-regulated (Figure 3B) in Cav1 KO fibroblasts were analyzed independently to identify which of these pathways were predominant in which particular group. In the group with up-regulated proteins, apoptosis signaling was the most significant pathway (p-value < 3×10^{-4}) with two molecules (Capns1 and Lmna) out of a possible 90 molecules associated with the pathway. This was followed by FAK signaling (p-value < 3.4×10^{-4}) and Integrin signaling (p-value < 1.6×10^{-3}), with two molecules (Capns1 and Actb) associated with the pathways out of a possible 104 and 205 molecules respectively. The proteins involved in KO phenotype pathways are all up-regulated suggesting an increased flux of these pathways in the KO phenotype. The group with down-regulated proteins had protein ubiquitination as the most significant pathway (p-value < 4×10^{-4}) with three down-regulated molecules (Hsp90b1, Hspa14 and Psmc2) associated with the pathway out of a possible 274 molecules. All the proteins involved in these pathways were down-regulated, which could suggest a decreased flux of these pathways in the KO phenotype.

To overcome the limitation of pathway-based analysis where not all genes have been assigned to a definitive pathway, we also interpreted the dataset of differentially expressed proteins in terms of a protein-interaction network. Another advantage of network analysis is that it offsets the bias that proteomics has against membrane proteins that limits their detectability. The differentially expressed proteins were uploaded and mapped to corresponding “gene objects” in the Ingenuity Pathways Knowledge Base (IPKB) in which the prior information used is a master gene interaction network curated from the scientific literature. The protein-interaction network significantly enriched in the dataset (p-value < 10^{-26}) containing all differentially expressed proteins is shown in Figure 4A and has a functional annotation associated with “cellular development,” which includes functions associated with the development and differentiation of cells. The intensity of the node color represents the degree of up- (red) or down-(green) regulation in fibroblasts. Validation of these nodes is an important step as they are major gene regulators and play central roles in mediating interactions among numerous less connected proteins and deletion of any of these nodes can perturb the network to a great extent [23].

Genetic depletion of caveolin-1 results in an increased expression of Caspn1 and Clec12b

Of all the differentially expressed proteins, actin was found to be the only one with known interactions with Cav1 (Figure 4A). Beta actin binds Cav1 in human platelets [24] and a fragment from Cav1α in Ht29 cells [25]. Notably, we identified two proteins that were differentially expressed and had no known interactions with Cav1 or any of the other differentially expressed proteins (Figure 4B). Src homology 2-B3 (Sh2b3), a key regulator of integrin-mediated cell motility in endothelial cells [26], was down-regulated in Cav1 KO cells by 1.8-fold. Similarly, Cav1 has been previously associated with integrin-mediated adhesion and signaling [11]. As a membrane adaptor, it links integrin to tyrosine kinase Fyn, which plays a role in integrin signaling and anchorage-independent growth[10]. We also found that C-type lectin domain family 12 member B protein (Clec12b), a receptor known to play an inhibitory role in myeloid cell function [27,28] was up-regulated in Cav1 KO cells by 1.6-

fold. To validate the proteomics results, Clec12b protein was observed by immunoblot to be increased by 1.5 fold following genetic depletion of Cav1 in cell lysates derived from MEFs (Figure 5A). Similarly, the level of Capns1 in Cav1 KO cells was increased by 2.8-fold over wild-type cells, which is consistent with our proteomics analysis result (see Figure 5A). To assess whether Cav1 causally influences the abundance of these proteins, Cav1 KO MEFs were infected with adenovirus encoding Cav1-GFP, and the cell lysates were subjected to SDS-PAGE and immunoblot analysis. As shown in Figure 5C, re-expression of Cav1 substantially suppressed Capns1 expression by 60% compared to either non-treated or GFP expressing cells. However, re-expression of Cav1 did not affect the expression of Clec12b (data not shown).

Caveolin-1 deficiency-induced apoptosis is mediated by Capns1

Our proteomics analysis result reveals that depletion of Cav1 results in up-regulation of Capns1 (Figure 2). In addition, both Cav1 and Capns1 have been shown to play a role in apoptosis [12,29–31] and cell migration [32–34]. Apoptosis plays an important role both in embryonic development and in maintaining homeostasis in adult tissue. These observations suggest that the sensitivity of Cav1 KO cells to apoptotic stimulation may be altered, although it has not been reported that calpain plays any role in Cav1 deficiency-induced apoptosis. A central component of the cell death machinery is a family of cysteine proteases, termed caspases [35]. Upon the receipt of death signals, caspases become activated, which subsequently cleave multiple cellular proteins leading to the demise of the cells. To test whether the sensitivity of Cav1 KO cells to apoptotic stimulation is affected, both wild-type and Cav1 KO cells were treated with or without 1 μM staurosporine, a commonly used apoptotic inducer,[29,36] and caspase 3 activity was measured. Although the basal activity of caspase 3 in Cav1 KO cells is lower than that in wild-type cells (open bars, Figure 5B), treatment of the cells with staurosporine increases substantially caspase 3 activity by more than 1.5-fold over that in wild-type cells (filled bars, Figure 5B). These results suggest that up-regulated expression of Capns1 may cause an increased sensitivity to apoptotic stimulation in Cav1 KO cells. To test this hypothesis, Cav1 KO cells were treated with Capns1 shRNA that knocked down the protein by more than 80% (Figure 6A). Suppression of Capns1 expression significantly inhibited caspase 3 activity by more than 50% compared to either non-treated or GFP expressing cells (Figure 6B). By combining proteomic and system biology analysis, we have identified Capns1 as a novel protein involved in apoptosis inducted by Cav1.

DISCUSSION

Viewing cell signaling networks as electrical circuits is a common analogy used to help understand how cells process information. In contrast to the flow of electrons or to the flow of mass in the case of metabolic networks, cell signaling networks represent the flow of cellular information by post-translationally modifying proteins and creating multi-protein complexes. To better understand the topology of a particular cell signaling network, a common approach is to remove nodes within a network and observe the functional consequence. Gene knockouts have become an essential tool for exploring the relationship between gene and phenotype. However, a common assumption is that the overall network

remains unaltered as nodes are removed from the network, i.e. a network exhibits simple or complicated characteristics. Here, we first considered the possibility that the signaling network associated with caveolin-1 - a protein that plays an important role in cell signaling and membrane trafficking - exhibits simple, complicated, or complex characteristics. To assess the local network properties associated with caveolin-1, we used a proteomics workflow to identify differences in protein expression between wild-type and caveolin-1 KO mouse embryonic fibroblasts. Specifically, we found that the local network associated with caveolin-1 exhibits complex characteristics in that loss of caveolin-1 altered the abundance of other proteins across the network. Similarly, various proteomics workflows have been used to gain insight into gene functions by comparing the KO and WT phenotypes[37–40]. Less biased proteomics workflows provide a more global view associated with a genetic knockout and help clarify the causal link between gene and biological function.

Using an integrated approach that combined genetic engineering, proteomics and computational systems biology tools to study a gene knockout, we have to a first approximation, determined the protein interactions and local network properties associated with caveolin-1. In this study, we have identified a number of proteins with an altered expression pattern on account of Cav1 knockout, which will help us refine our understanding the role of Cav1 in cell signaling and membrane trafficking. Our findings suggest that the expression of Capns1, Sh2b3 and Clec12b is dependent on Cav1, as Cav1 depletion up-regulates Capns1 and Clec12b expression and down-regulates Sh2b3 expression. Both Sh2b3 and Cav1 have been shown to play a role in integrin-mediated cell migration[10,26]. Similarly, Clec12b and Cav1 are both involved in angiogenesis[28,41–43]. Sh2b3 and Clec12b have no known interactions with Cav1 or any of the other differentially expressed proteins as evident from the protein interaction map. Thus, our results suggest that Sh2b3 and Clec12b may mediate Cav1 functions and have the potential to interact with Cav1, although direct validation of these interactions remains. More importantly, we have shown that the sensitivity of Cav1 KO cells to apoptotic stimulation is enhanced and that calpain small subunit 1 (Capns1) directly influences the sensitivity of cells to apoptotic stimuli.

Here we have shown using an unbiased proteomics approach that a knockout phenotype not only lacks the product of the particular gene, but exhibits a number of phenotypical changes that are altered to compensate for the mutation, which might not necessarily related to the function of gene of interest and hence easily overlooked. In other words, the signaling network containing caveolin-1 behaves as a complex system. On the surface, this observation may seem to conflict with findings that biological systems have evolved to be functionally robust to small perturbations in protein activity/abundance around their homeostatic set points [44,45]. However, knocking out a protein is not a small perturbation. Collectively, the identified proteins altered in response to caveolin-1 knockout may comprise the local network that buffers the functional response against slight variation in protein abundance. Specifically, Cav1 KO increases the abundance of Capns1 and the sensitivity of cells to apoptotic stimuli. In independent experiments, we show that the sensitivity to apoptotic stimuli is proportional to Capns1 abundance. Assuming that the dose-response relationships are linear, the increase in Capns1 may buffer a reduction in Cav1 abundance to help maintain the sensitivity of a cell to apopotic stimuli. Moreover,

these results suggest that the role that a protein plays within a perturbed network may change, confounding inferring simple gene-phenotype relationships from gene knock-out experiments.

CONCLUSION

Gene knockouts result in differential expression of several other proteins, some of which might be contributing to the resulting phenotype in addition to the target gene. These contributing proteins, some of which might be possible interaction partners of the target gene, are often overlooked while conducting targeted studies. Analyzing the differences between WT and Cav1 KO phenotypes using an unbiased proteomics approach, we have identified Sh2b3 and Clec12b as putative novel interaction partners of Cav1. Our results also suggest that Capns1 may help buffer changes in caveolin-1 in regulating the cell response to apoptotic stimuli.

Supplementary Material

Refer to Web version on PubMed Central for supplementary material.

Acknowledgments

We thank Dr. John Barnett (Department of Microbiology, Immunology and Cell Biology, West Virginia University School of Medicine) for generously providing 2-DE equipment and Aviva Systems Biology (San Diego, CA) for providing antibody against Capns1. This work was supported in part by grants from the American Cancer Society (JL), the National Science Foundation (DJK) and the National Cancer Institute (DJK).

Financial disclosure

This work was supported by the grants from American Cancer Society (CSM-115295 to JL), National Science Foundation (CAREER 1053490 to DJK) and the National Cancer Institute (R15CA123123 to DJK). The content is solely the responsibility of the authors and does not necessarily represent the official views of the American Cancer Society, the National Cancer Institute, the National Institutes of Health, or the National Science Foundation. The funders had no role in study design, data collection and analysis, decision to publish, or preparation of the manuscript.

The abbreviations used are

Cav1	caveolin-1
Capns1	calpain small subunit 1
IPA	Ingenuity Pathway Analysis
MEFs	mouse embryonic fibroblasts
2-DE	two-dimensional electrophoresis
PMF	peptide mass fingerprint
IPKB	Ingenuity Pathways Knowledge Base

References

1. Anderson RG. Caveolae: Where Incoming and Outgoing Messengers Meet. 1993; 90:10909–10913.

2. Lisanti MP, Scherer PE, Tang Z, Sargiacomo M. Caveolae, Caveolin and Caveolin-Rich Membrane Domains: a Signalling Hypothesis. 1994; 4:231–235.
3. Liu P, Rudick M, Anderson RG. Multiple Functions of Caveolin-1. J. Biol. Chem. 2002; 277:41295–41298. [PubMed: 12189159]
4. Martin S, Parton RG. Caveolin, Cholesterol, and Lipid Bodies. Semin. Cell Dev. Biol. 2005; 16:163–174. [PubMed: 15797827]
5. Way M, Parton RG. M-Caveolin, a Muscle-Specific Caveolin-Related Protein. FEBS Lett. 1995; 376:108–112. [PubMed: 8521953]
6. Song KS, Scherer PE, Tang Z, Okamoto T, Li S, Chafel M, Chu C, Kohtz DS, Lisanti MP. Expression of Caveolin-3 in Skeletal, Cardiac, and Smooth Muscle Cells. Caveolin-3 Is a Component of the Sarcolemma and Co-Fractionates With Dystrophin and Dystrophin-Associated Glycoproteins. 1996; 271:15160–15165.
7. Li S, Couet J, Lisanti MP. Src Tyrosine Kinases, Galpha Subunits, and H-Ras Share a Common Membrane-Anchored Scaffolding Protein, Caveolin. Caveolin Binding Negatively Regulates the Auto-Activation of Src Tyrosine Kinases. 1996; 271:29182–29190.
8. Couet J, Li S, Okamoto T, Ikezu T, Lisanti MP. Identification of Peptide and Protein Ligands for the Caveolin-Scaffolding Domain. Implications for the Interaction of Caveolin With Caveolae-Associated Proteins. 1997; 272:6525–6533.
9. Okamoto T, Schlegel A, Scherer PE, Lisanti MP. Caveolins, a Family of Scaffolding Proteins for Organizing "Preassembled Signaling Complexes" at the Plasma Membrane. 1998; 273:5419–5422.
10. Wary KK, Mariotti A, Zurzolo C, Giancotti FG. A Requirement for Caveolin-1 and Associated Kinase Fyn in Integrin Signaling and Anchorage-Dependent Cell Growth. 1998; 94:625–634.
11. Wei Y, Yang X, Liu Q, Wilkins JA, Chapman HA. A Role for Caveolin and the Urokinase Receptor in Integrin-Mediated Adhesion and Signaling. 1999; 144:1285–1294.
12. Zundel W, Swiersz LM, Giaccia A. Caveolin 1-Mediated Regulation of Receptor Tyrosine Kinase-Associated Phosphatidylinositol 3-Kinase Activity by Ceramide. 2000; 20:1507–1514.
13. Mercier I, Jasmin JF, Pavlides S, Minetti C, Flomenberg N, Pestell RG, Frank PG, Sotgia F, Lisanti MP. Clinical and Translational Implications of the Caveolin Gene Family: Lessons From Mouse Models and Human Genetic Disorders. Lab Invest. 2009; 89:614–623. [PubMed: 19333235]
14. Muller U. Ten Years of Gene Targeting: Targeted Mouse Mutants, From Vector Design to Phenotype Analysis. 1999; 82:3–21.
15. Colot HV, Park G, Turner GE, Ringelberg C, Crew CM, Litvinkova L, Weiss RL, Borkovich KA, Dunlap JC. A High-Throughput Gene Knockout Procedure for Neurospora Reveals Functions for Multiple Transcription Factors. 2006; 103:10352–10357.
16. Skarnes WC, Rosen B, West AP, Koutsourakis M, Bushell W, Iyer V, Mujica AO, Thomas M, Harrow J, Cox T, Jackson D, Severin J, Biggs P, Fu J, Nefedov M, de Jong PJ, Stewart AF, Bradley A. A Conditional Knockout Resource for the Genome-Wide Study of Mouse Gene Function. 2011; 474:337–342.
17. Zambrowicz BP, Sands AT. Knockouts Model the 100 Best-Selling Drugs--Will They Model the Next 100? 2003; 2:38–51.
18. Amaral LAN, Ottino JN. 2004; 59:1653–1666.
19. Hanahan D, Weinberg RA. Hallmarks of Cancer: the Next Generation. Cell. 2011; 144:646–674. [PubMed: 21376230]
20. Lazebnik Y. Can a Biologist Fix a Radio?--Or, What I Learned While Studying Apoptosis. Cancer Cell. 2002; 2:179–182. [PubMed: 12242150]
21. Klinke DJ. Signal Transduction Networks in Cancer: Quantitative Parameters Influence Network Topology. Cancer Res. 2010; 70:1773–1782. [PubMed: 20179207]
22. Gerlai R. Gene-Targeting Studies of Mammalian Behavior: Is It the Mutation or the Background Genotype? 1996; 19:177–181.
23. Zotenko E, Mestre J, O'Leary DP, Przytycka TM. Why Do Hubs in the Yeast Protein Interaction Network Tend to Be Essential: Reexamining the Connection Between the Network Topology and Essentiality. PLoS. Comput. Biol. 2008; 4:e1000140. [PubMed: 18670624]

24. Lasfargues EY, Coutinho WG, Redfield ES. J.Natl.Cancer Inst. 1978; 61:961–978. [PubMed: 309009]
25. Doucey MA, Bender FC, Hess D, Hofsteenge J, Bron C. Caveolin-1 Interacts With the Chaperone Complex TCP-1 and Modulates Its Protein Folding Activity. 2006; 63:939–948.
26. Takizawa H, Eto K, Yoshikawa A, Nakauchi H, Takatsu K, Takaki S. Growth and Maturation of Megakaryocytes Is Regulated by Lnk/Sh2b3 Adaptor Protein Through Crosstalk Between Cytokine- and Integrin-Mediated Signals. Exp Hematol. 2008; 36:897–906. [PubMed: 18456388]
27. Hoffmann SC, Schellack C, Textor S, Konold S, Schmitz D, Cerwenka A, Pflanz S, Watzl C. Identification of CLEC12B, an Inhibitory Receptor on Myeloid Cells. J Biol Chem. 2007; 282:22370–22375. [PubMed: 17562706]
28. Murdoch C, Muthana M, Coffelt SB, Lewis CE. The Role of Myeloid Cells in the Promotion of Tumour Angiogenesis. Nat Rev Cancer. 2008; 8:618–631. [PubMed: 18633355]
29. Liu J, Lee P, Galbiati F, Kitsis RN, Lisanti MP. Caveolin-1 Expression Sensitizes Fibroblastic and Epithelial Cells to Apoptotic Stimulation. Am J Physiol Cell Physiol. 2001; 280:823–835.
30. Demarchi F, Schneider C. The Calpain System As a Modulator of Stress/Damage Response. 2007; 6:136–138.
31. Kasper M, Barth K. Bleomycin and Its Role in Inducing Apoptosis and Senescence in Lung Cells - Modulating Effects of Caveolin-1. Curr Cancer Drug Targets. 2009; 9:341–353. [PubMed: 19442053]
32. Beardsley A, Fang K, Mertz H, Castranova V, Friend S, Liu J. Loss of Caveolin-1 Polarity Impedes Endothelial Cell Polarization and Directional Movement. 2005; 280:3541–3547.
33. Sun XH, Flynn DC, Castranova V, Millecchia LL, Beardsley AR, Liu J. Identification of a Novel Domain at the N Terminus of Caveolin-1 That Controls Rear Polarization of the Protein and Caveolae Formation. 2007; 282:7232–7241.
34. Pamonsinlapatham P, Gril B, Dufour S, Hadj-Slimane R, Gigoux V, Pethe S, L'hoste S, Camonis J, Garbay C, Raynaud F, Vidal M. Capns1, a New Binding Partner of RasGAP-SH3 Domain in K-Ras(V12) Oncogenic Cells: Modulation of Cell Survival and Migration. Cell Signal. 2008; 20:2119–2126. [PubMed: 18761085]
35. Thornberry NA, Lazebnik Y. Caspases: Enemies Within. Science. 1998; 281:1312–1316. [PubMed: 9721091]
36. Bertrand R, Solary E, O'Connor P, Kohn KW, Pommier Y. Induction of a Common Pathway of Apoptosis by Staurosporine. Exp Cell Res. 1994; 211:314–321. [PubMed: 8143779]
37. Chivasa S, Tome DF, Hamilton JM, Slabas AR. Proteomic Analysis of Extracellular ATP-Regulated Proteins Identifies ATP Synthase Beta-Subunit As a Novel Plant Cell Death Regulator. 2011; 10:M110.
38. Jin H, Hu R, Cheng Y, Yang F, Zhou X, Li X, Yang PY. Differential Protein Expression Level Identification by Knockout of 14-3-3tau With SiRNA Technique and 2DE Followed MALDI-TOF-TOF-MS. 2011; 136:401–406.
39. Magdeldin S, Li H, Yoshida Y, Enany S, Zhang Y, Xu B, Fujinaka H, Yaoita E, Yamamoto T. Comparison of Two Dimensional Electrophoresis Mouse Colon Proteomes Before and After Knocking Out Aquaporin 8. 2010; 73:2031–2040.
40. Azkargorta M, Arizmendi JM, Elortza F, Alkorta N, Zubiaga AM, Fullaondo A. Differential Proteome Profiles in E2F2-Deficient T Lymphocytes. 2006; 6(Suppl 1):S42–S50.
41. Liu J, Wang XB, Park DS, Lisanti MP. Caveolin-1 Expression Enhances Endothelial Capillary Tubule Formation. 2002; 277:10661–10668.
42. Woodman SE, Ashton AW, Schubert W, Lee H, Williams TM, Medina FA, Wyckoff JB, Combs TP, Lisanti MP. Caveolin-1 Knockout Mice Show an Impaired Angiogenic Response to Exogenous Stimuli. Am. J. Pathol. 2003; 162:2059–2068. [PubMed: 12759260]
43. Fang K, Fu W, Beardsley AR, Sun X, Lisanti MP, Liu J. Overexpression of Caveolin-1 Inhibits Endothelial Cell Proliferation by Arresting the Cell Cycle at G0/G1 Phase. 2007; 6:199–204.
44. Goentoro L, Kirschner MW. Evidence That Fold-Change, and Not Absolute Level, of Beta-Catenin Dictates Wnt Signaling. Mol. Cell. 2009; 36:872–884. [PubMed: 20005849]
45. Goentoro L, Shoval O, Kirschner MW, Alon U. The Incoherent Feedforward Loop Can Provide Fold-Change Detection in Gene Regulation. Mol. Cell. 2009; 36:894–899. [PubMed: 20005851]

46. Kulkarni YM, Suarez V, Klinke DJ. Inferring Predominant Pathways in Cellular Models of Breast Cancer Using Limited Sample Proteomic Profiling. BMC. Cancer. 2010; 10:291. [PubMed: 20550684]

47. Benjamini Y, Hochberg Y. Journal of the Royal Statistical Society.Series B (Methodological). 1995; 57:289–300.

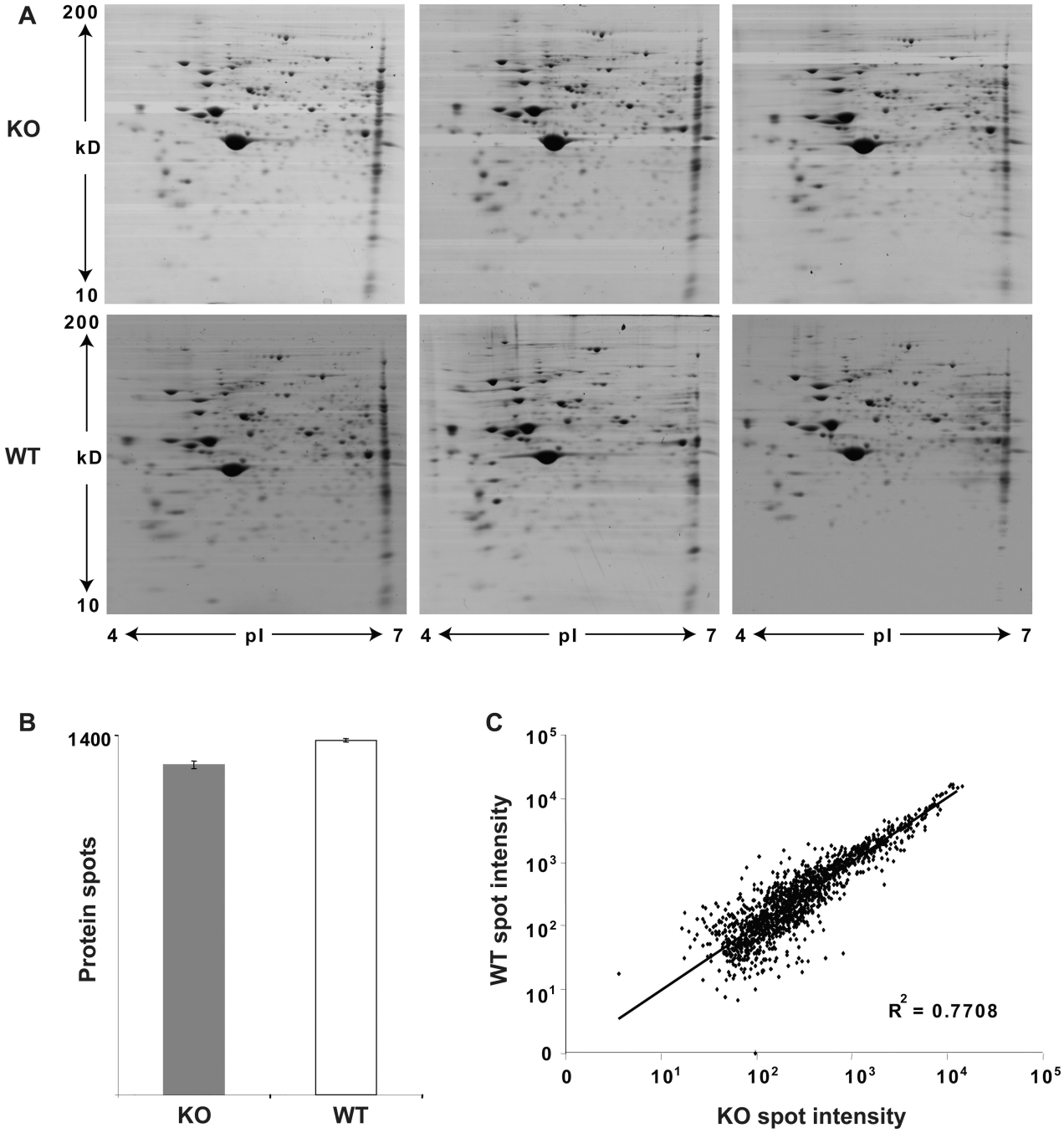

Figure 1.

(A) Technical replicates showing 2-D proteomic profiles of Cav1 KO and WT MEFs. The first dimension was resolved on IPG strip 4–7, 7cm. The second dimension is a 12% SDS-PAGE spanning molecular weight region of 10–200 kDa. 2-D gels were stained with coomassie blue and scanned using Typhoon 9400 scanner. (B) Quantitative image analysis using Ludesi REDFIN reveals the gel reproducibility and protein loading with no significant difference in the number of identified protein spots on the gel replicates across each cell line. Error bars represent S.E.M. (C) Scatter plots of average normalized intensities are

plotted on a logarithmic scale for matching protein spots showing the dynamic range of spot detection and correlation for the WT versus Cav1 KO MEFs.

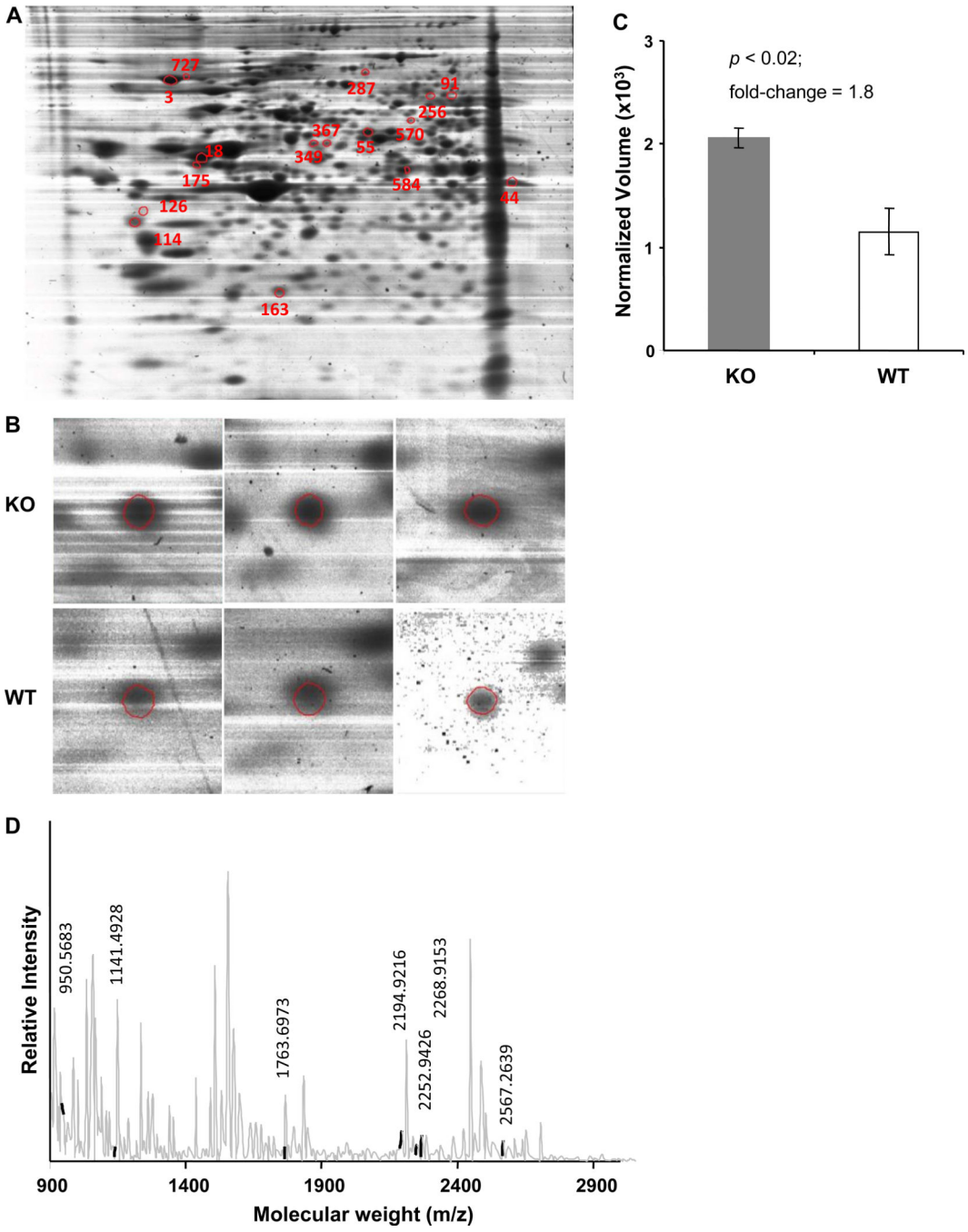

Figure 2.

(A) Using all of the 2D gel images shown in Figure 1A, a composite image was generated by Ludesi Redfin image analysis software that shows the locations of all 16 protein spots that are differentially expressed between WT and Cav1 KO MEFs. Spots are numbered arbitrarily by the software. (B) Montage showing differential expression of Capns1 on each gel across both groups (identified spot border is in red). (C) Densitometric quantitation of the normalized volume of Capns1 on each gel with the associated fold-change and corresponding *p*-value. (D) Mass spectra for each peptide digest was acquired between mass

values of 800 and 3000, deisotoped using PLGS2.1 and submitted for peptide mass fingerprinting. The mass spectrum is shown for Capns1 with the peptide mass values that contributed towards successful identification of the protein indicated in bold and numbered on the spectrum.

A

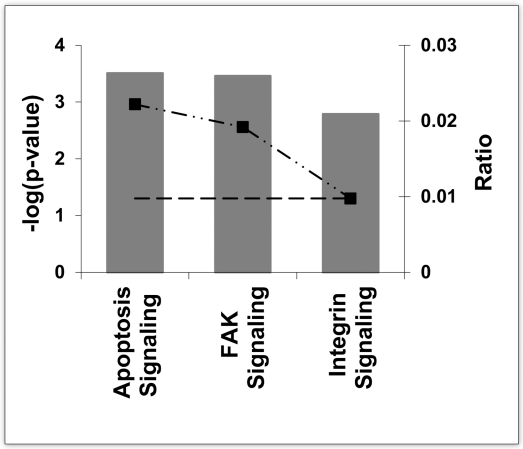

Pathway	Associated Genes
Apoptosis Signaling	CAPNS1, LMNA
FAK Signaling	CAPNS1, ACTB
Integrin Signaling	CAPNS1, ACTB

B

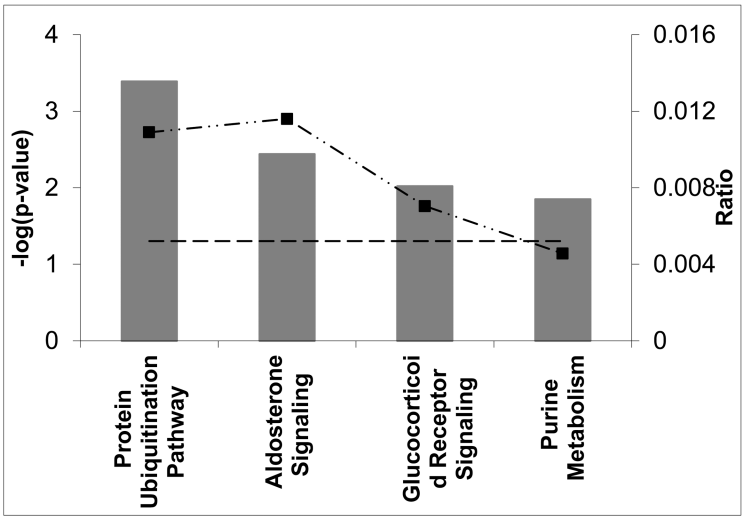

Pathway	Associated Genes
Protein Ubiquitination Pathway	HSP90B1, HSPA14, PSMC2
Aldosterone Signaling	HSP90B1, HSPA14
Glucocorticoid Receptor Signaling	HSP90B1, HSPA14
Purine Metabolism	ATP5B, PSMC2

Figure 3.

Significant canonical pathways ($p < 0.05$) for proteins differentially expressed between Cav1 KO and WT MEFs. The negative of the $\log_{10}$ (p-value) (long dash) and ratio (number of focus molecules involved in the pathway/total number of molecules in the pathway; long dash dot joined by squares) are plotted on the primary and secondary Y-axis respectively. Panel A, Canonical pathways resulting from proteins up-regulated in Cav1 deficient MEFs. Panel B, Canonical pathways resulting from proteins down-regulated in Cav1 KO MEFs.

A

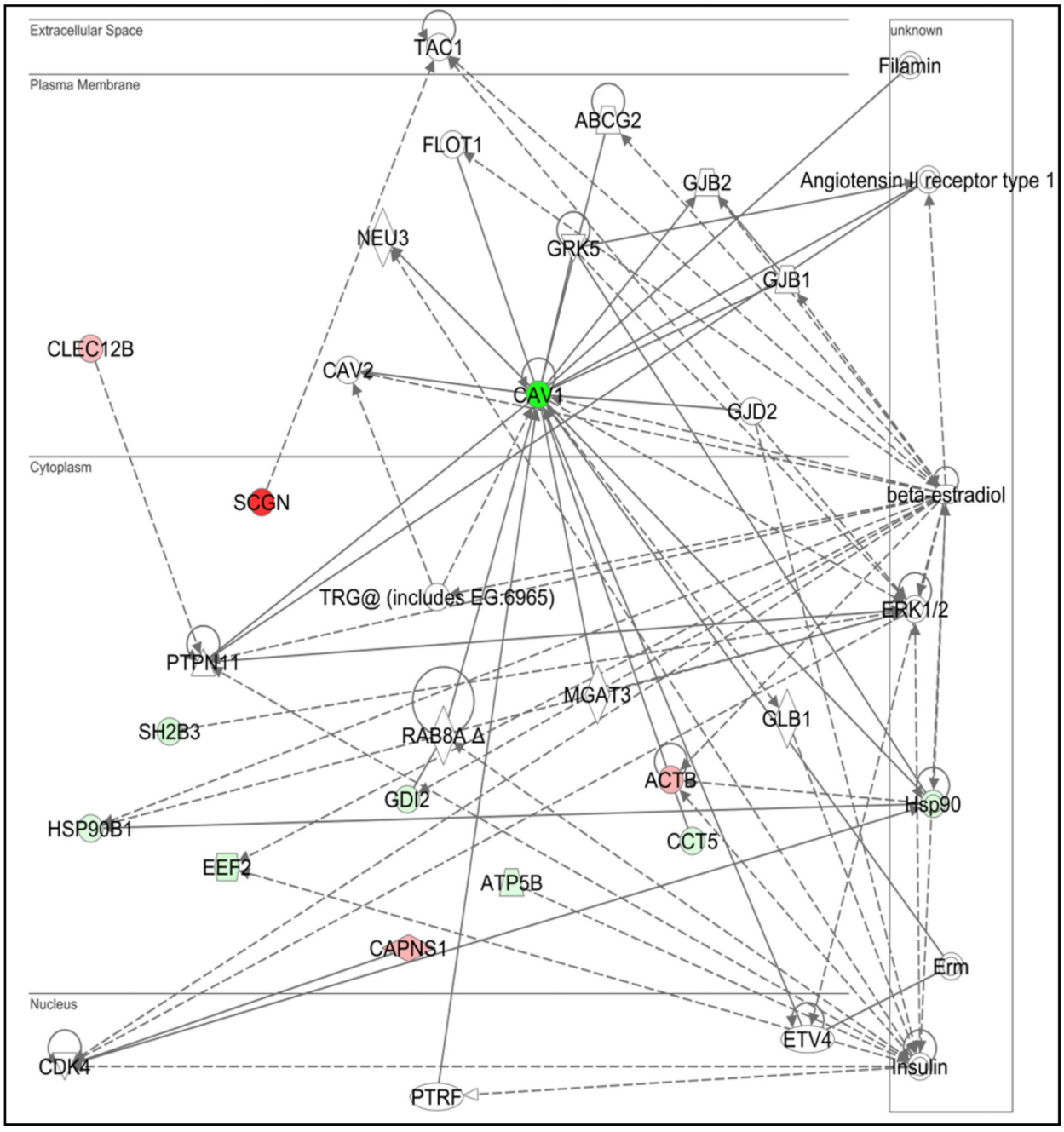

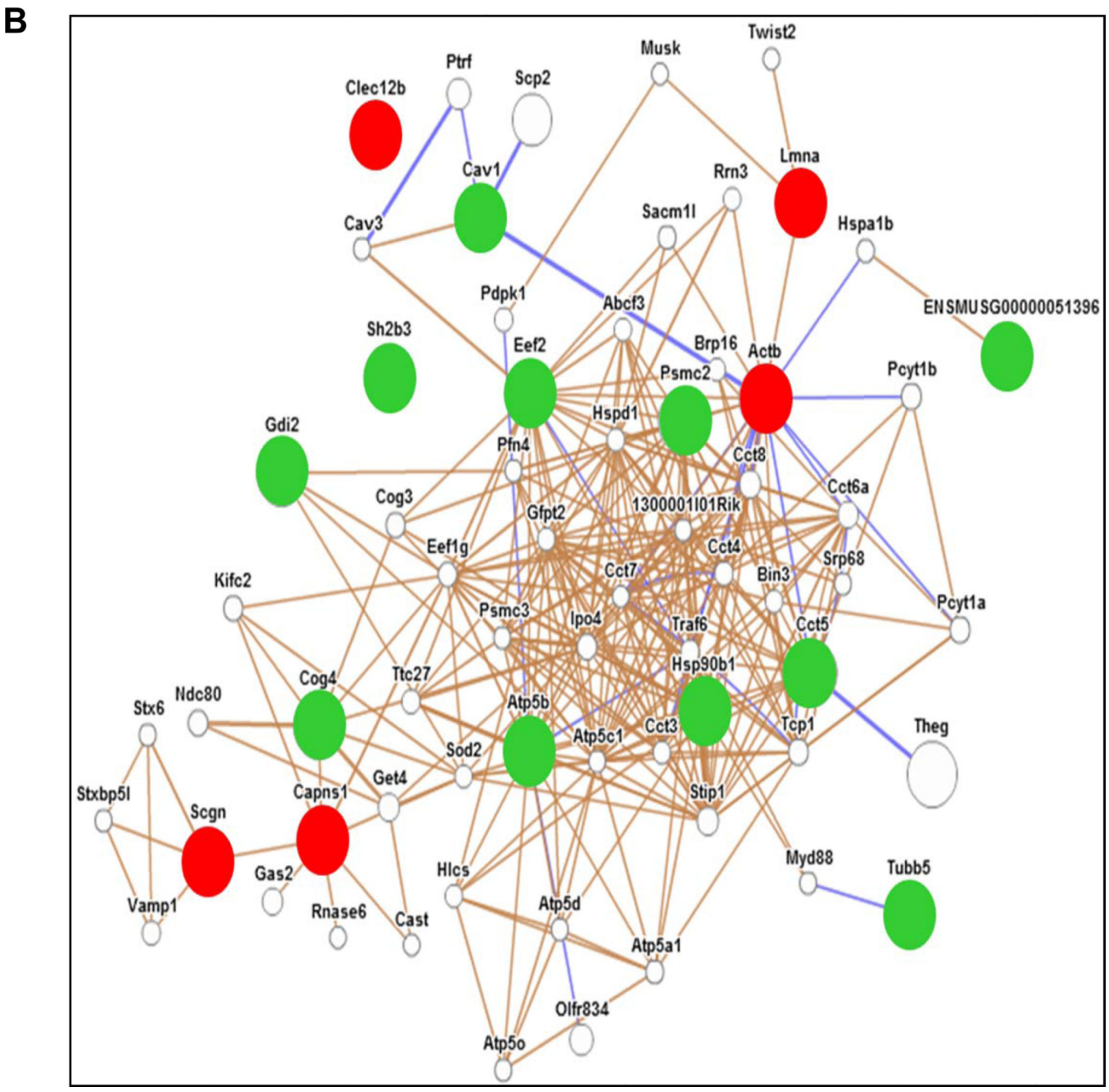

Figure 4.

Proteins differentially expressed in Cav1 KO and WT MEFs were overlaid onto a global molecular network developed from information contained in the Ingenuity Knowledge Base (IKB). Genes or gene products are represented as nodes, and the biological relationship between two nodes is represented as an edge (line). Solid lines indicate a direct relationship and dashed lines indicate an indirect relationship between nodes. The intensity of the node color represents the degree of up-regulation in KO cells- red (up-regulation) and green (down-regulation). White nodes represent the IKB molecules associated with focus genes. Network reflects (A) Interaction network for differentially expressed proteins between Cav1

KO and WT cells (Network function: Cellular development, $p < 10^{-26}$); and (B) GeneMania network showing physical (blue lines) and predicted (brown lines) interactions between the differentially expressed proteins and other gene products. Red nodes are proteins up-regulated in Cav1 KO cells, green nodes are proteins down-regulated in KO cells, and the white nodes are gene products known to interact with the data set. Hanging nodes indicate no known interaction with other nodes in the network.

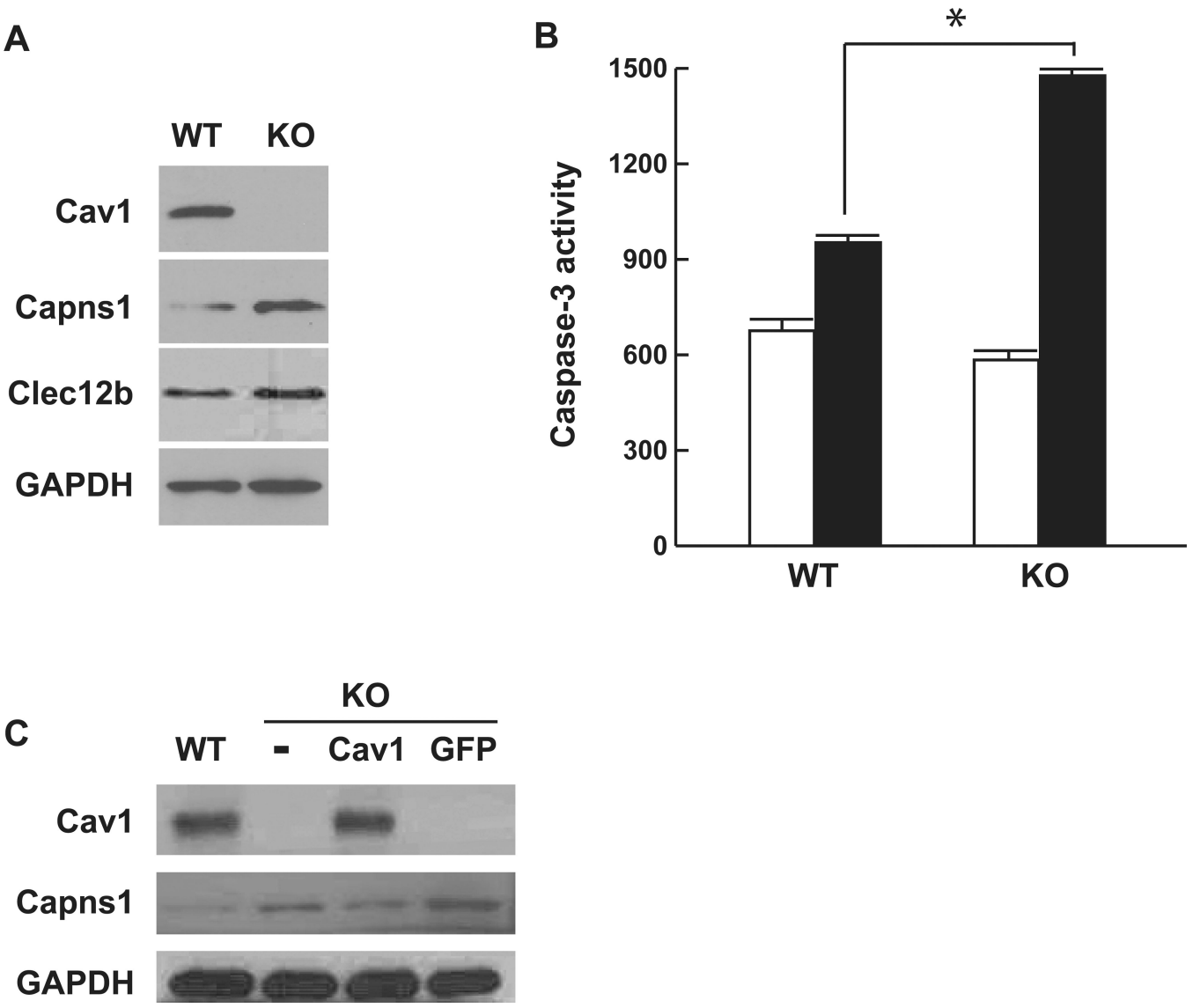

Figure 5. Up-regulation of Capns 1 expression and enhancement of apoptosis in caveolin-1 KO MEFs

(A) WT and Cav1 KO MEFs were lysed and immunoblotted with the antibodies against the proteins as show in the figure. The same membrane was reprobed with the antibody against GAPDH for equal protein loading. Note that calpain small subunit 1 (Capns1) and Clec12b are up-regulated in Cav1 KO cells. (B) WT and Cav1 KO MEFs were incubated with (filled bars) or without (open bars) staurosporine (1 μM) in normal growth medium for 3 hours. Caspase 3-like proteolytic activity was determined using caspase 3 fluorescent assay kit. The data are the means ± SD. *, $P<0.001$. (C) Cav1 KO MEFs were infected with adenovirus encoding either Cav1-GFP (Cav1) or GFP alone (GFP) for 24 hours. Cell were lysed and immunoblotted with the antibodies against the proteins as shown in the figure. The same membrane was reprobed with the antibody against GAPDH for equal protein loading.

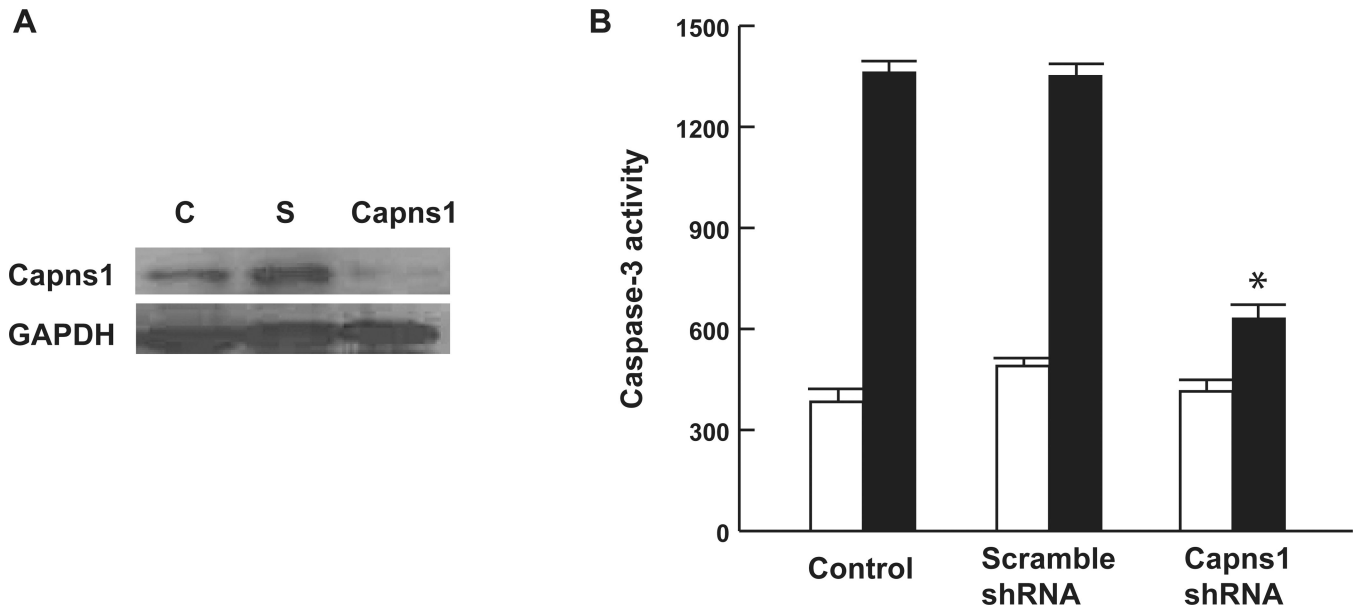

Figure 6. Knock down of Capns1 inhibits apoptotic activity in caveolin-1 KO MEFs

(A) Cav1 KO MEFs were infected with lentivirus encoding either Capns1 shRNA (Capns1) or scramble shRNA (S) for 72 hours. Cell were lysed and immunoblotted with the antibodies against Capns1. The same membrane was reprobed with the antibody against GAPDH for equal protein loading. Note that the level of Capns1 protein expression was specifically knocked down by Capns1 shRNA. (B) Cav1 KO MEFs infected with Capns1 shRNA as in (A) were treated with staurosporine, and caspase 3-like activity was determined as in (B) of Fig. 5. Note that knock down of Capns1 results in substantial decrease in caspase 3 activity by more than 50% compared to non-treated or scramble shRNA treated cells. The data are the means ± SD. *, $P<0.001$.

Table 1

List of proteins that were differentially expressed and formed the dataset for IPA analysis are listed along with the associated theoretical and observed MW and pI, fold-change and *p*-value.

ID	Protein	Gene ID	Theoretical		Observed		Upregulated in	Fold-change	*p*
			MW	pI	MW	pI			
3	Endoplasmin	Hsp90b1	90	4.7	91	4.7	WT	1.51	0.01
18	Tubulin beta-5 chain	Tubb5	50	4.8	58	4.9	WT	1.50	0.01
44	Actin, cytoplasmic 1	Actb	42	5.3	50	6.8	KO	1.84	0.02
55	T-complex protein 1 subunit epsilon	Cct5	59	5.7	68	5.9	WT	1.59	0.007
91	Prelamin-A/C	Lmna	74	6.5	84	6.4	KO	2.58	0.01
114	C-type lectin domain family 12 member B	Clec12b	31	5	40	4.5	KO	1.64	0.01
126	Secretagogin	Scgn	32	5	42	4.5	KO	4.95	3.5E-7
163	Calpain small subunit 1	Capns1	28	5.4	27	5.4	KO	1.8	0.01
175	ATP synthase subunit beta, mitochondrial	Atp5b	52	5	56	4.9	WT	1.52	0.04
256	No identification						KO	1.95	0.04
287	Elongation factor 2	Eef2	95	6.4	96	5.9	WT	1.86	0.02
349	Heat shock 70 kDa protein 14	Hspa14	55	5.6	63	5.6	WT	2.93	0.01
367	26S protease regulatory subunit 7	Psmc2	49	5.7	63	5.7	WT	2.30	0.04
570	SH2B adapter protein 3	Sh2b3	60	6.7	72	6.2	WT	1.85	0.02
584	Rab GDP dissociation inhibitor beta	Gdi2	51	5.9	54	6.2	WT	1.69	7.5E-4
727	Conserved oligomeric Golgi complex subunit 4	Cog4	89	5	94	4.8	WT	1.99	0.003